

RSC Advances



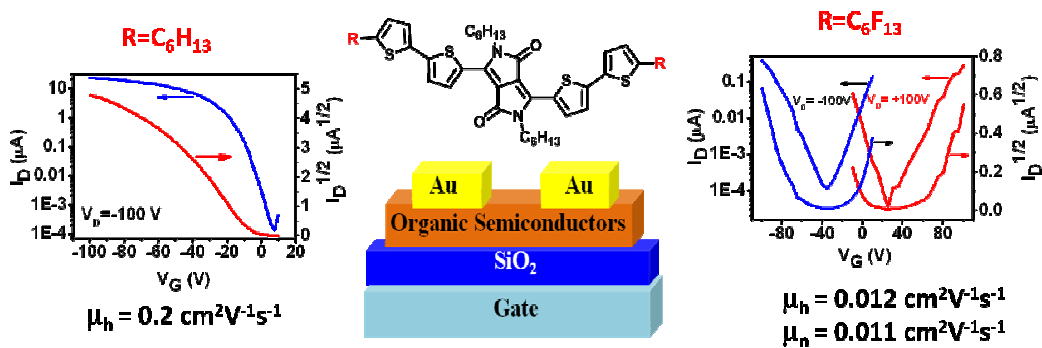
This is an *Accepted Manuscript*, which has been through the Royal Society of Chemistry peer review process and has been accepted for publication.

Accepted Manuscripts are published online shortly after acceptance, before technical editing, formatting and proof reading. Using this free service, authors can make their results available to the community, in citable form, before we publish the edited article. This *Accepted Manuscript* will be replaced by the edited, formatted and paginated article as soon as this is available.

You can find more information about *Accepted Manuscripts* in the [Information for Authors](#).

Please note that technical editing may introduce minor changes to the text and/or graphics, which may alter content. The journal's standard [Terms & Conditions](#) and the [Ethical guidelines](#) still apply. In no event shall the Royal Society of Chemistry be held responsible for any errors or omissions in this *Accepted Manuscript* or any consequences arising from the use of any information it contains.

TOC



Two novel diketopyrrolopyrrole (DPP) small molecules **DPPTT-F** and **DPPTT-H** were synthesized and characterized. Thin film transistor characteristics showed **DPPTT-H** exhibited p-channel behavior, and **DPPTT-F** displayed ambipolar characteristics with balanced hole and electron mobility in air.

Cite this: DOI: 10.1039/c0xx00000x

www.rsc.org/xxxxxx

ARTICLE TYPE

Perfluorohexyl Containing Diketopyrrolopyrrole (DPP) Small Molecule for High Performance Ambipolar Transistors with Balanced Hole and Electron Mobility

Yuanyuan Wang,^{a,b,†} Qiuliu Huang,^{a,†} Zhiqiang Liu,^{b,*} Hongxiang Li^{a,*}

Received (in XXX, XXX) Xth XXXXXXXXX 20XX, Accepted Xth XXXXXXXXX 20XX
DOI: 10.1039/b000000x

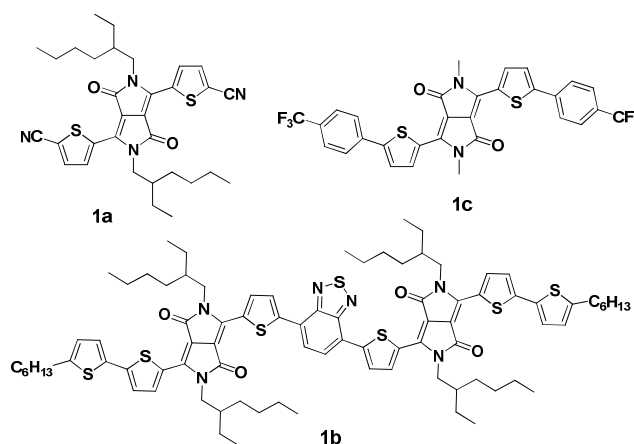
Two novel diketopyrrolopyrrole (DPP) small molecules **DPPTT-F** and **DPPTT-H** were synthesized. With the change of substituent from hexyl to perfluorohexyl, the HOMO and LUMO energy levels of **DPPTT-F** lowered, but the bandgap of **DPPTT-H** and **DPPTT-F** was nearly the same, which was proved by absorption spectra and electrochemistry. Thin film transistor characteristics showed **DPPTT-H** exhibited p-channel behavior with a hole mobility about $0.2 \text{ cm}^2 \text{V}^{-1} \text{s}^{-1}$, while **DPPTT-F** displayed ambipolar characteristics with balanced hole and electron mobility in air. The mobility of **DPPTT-F** was $0.012 \text{ cm}^2 \text{V}^{-1} \text{s}^{-1}$ for hole and $0.011 \text{ cm}^2 \text{V}^{-1} \text{s}^{-1}$ for electron. The microstructure and morphology of the thin films were also investigated. All these results demonstrated the unique property of perfluoroalkyl chains and their potential application in high performance organic ambipolar semiconductors.

Introduction

Ambipolar organic semiconductors, which can fabricate light-emitting transistors and complementary metal-oxide semiconductor (CMOS)-like logic circuits in simple way at low cost, have attracted great attentions recently.¹⁻⁴ Though continuous progress has been made,⁵⁻⁷ the lack of ambient stable and high performance ambipolar semiconductors is still one of the bottlenecks for their practical applications, especially the one with balanced hole and electron mobility. Hence, it is vital and needed to develop novel high performance ambipolar semiconductors with balanced hole and electron mobility under ambient condition.

Diketopyrrolopyrrole (DPP) has fused planar structure and is an excellent building block for high performance polymer semiconductors.⁸⁻¹¹ Recently, DPP based small molecules have caught the attentions owing to their well defined structure and promising charge transport performance.¹²⁻¹⁶ For instance, vacuum deposited thin films of DPP derivative **1a** (Scheme 1) showed a high hole mobility of $0.7 \text{ cm}^2 \text{V}^{-1} \text{s}^{-1}$ and a current on/off ratio of 10^6 under ambient conditions.¹⁴ Till now, most of the reported DPP based small molecules exhibited p-channel behavior, ambipolar materials are rarely reported and most of them are measured under vacuum or in inert atmosphere. Compound **1b** (Scheme 1) displayed one of the highest ambipolar performance among DPP based small molecules with balanced electron and hole mobility about $10^{-3} \text{ cm}^2/\text{Vs}$ in vacuum by using Au as source and drain electrodes.¹⁶

It is well known that the fluorine-contained substituents can effectively lower the energy level of molecules and influence their orientation in the solid state, and thus affect the charge-



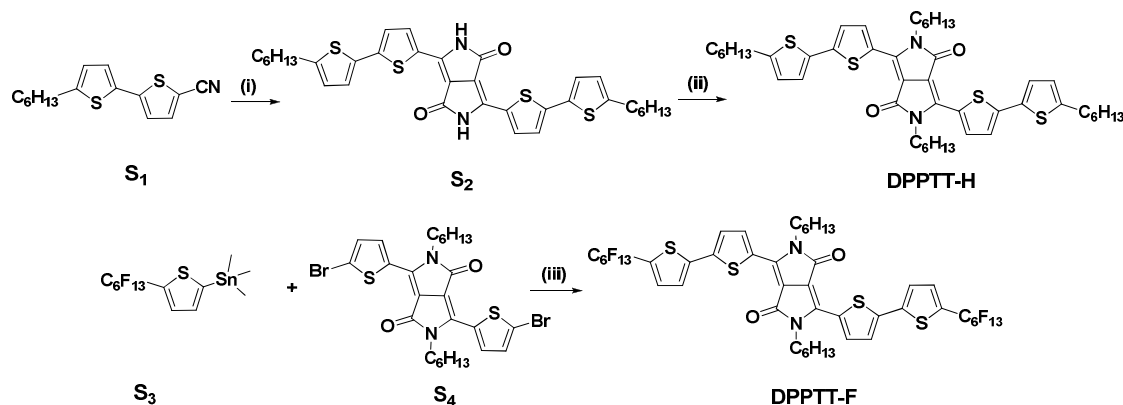
Scheme 1. Some representative DPP-containing small molecular organic semiconductors

transport behavior of materials.¹⁷⁻²⁰ However, no much attentions has been paid to fluorine-containing DPP based small molecules. Y. Suna firstly introduced fluorine substituents into DPP based small molecules and synthesized compound **1c** (Scheme 1).²⁰ Thin film transistors of **1c** displayed ambipolar characteristics. Though the performance of **1c** was not high (electron mobility: $10^{-4} \text{ cm}^2 \text{V}^{-1} \text{s}^{-1}$, hole mobility: $10^{-5} \text{ cm}^2 \text{V}^{-1} \text{s}^{-1}$), it can be operated in ambient condition which is crucial to fabricate ambipolar transistors easily with low cost. Herein, two novel DPP derivatives **DPPTT-F** and **DPPTT-H** (Scheme 2) were successfully synthesized. Both compounds have same conjugation backbone, but their alkyl chain substituents are different. The alkyl chain substituents are hexyl for **DPPTT-H** and perfluorohexyl for **DPPTT-F**. Absorption spectra and electrochemistry results showed the replacement of hexyl with

Cite this: DOI: 10.1039/c0xx00000x

www.rsc.org/xxxxxx

ARTICLE TYPE



Scheme 2. Synthetic routes of **DPPTT-H** and **DPPTT-F**. Reagents and conditions: (i) $(\text{CH}_2)_2(\text{COOMe})_2$, $\text{NaOC}(\text{CH}_3)_2(\text{CH}_2\text{CH}_3)$, *tert*-amyl alcohol, 110 °C, 3h; (ii) K_2CO_3 , DMF, $\text{BrC}_6\text{H}_{13}$; (iii) $\text{Pd}(\text{PPh}_3)_4$, toluene, 130 °C, 20h.

perfluorohexyl lowered the HOMO and LUMO energy levels of **DPPTT-F**, but the HOMO-LUMO energy bandgaps of **DPPTT-H** and **DPPTT-F** were nearly the same. Thin film transistor characteristics showed **DPPTT-H** exhibited p-channel behavior with hole mobility about $0.2 \text{ cm}^2\text{V}^{-1}\text{s}^{-1}$, while **DPPTT-F** based transistors showed ambipolar properties with balanced hole and electronic mobilities in air. The maximum hole and electron mobility of **DPPTT-F** were $0.012 \text{ cm}^2\text{V}^{-1}\text{s}^{-1}$ and $0.011 \text{ cm}^2\text{V}^{-1}\text{s}^{-1}$, respectively, one of the highest value for DPP based ambipolar transistors in air. Their thin film microstructure and morphology were also investigated.

Experimental section

Materials synthesis

All reactions were carried out under nitrogen atmosphere unless stated otherwise. The reagents were purchased from commercial suppliers and were used directly without further purification unless otherwise noted. Compounds **S1**, **S3** and **S4** were synthesized according to the literature.²¹⁻²⁴

Synthesis of compound S2

A mixture of **S1** (1.10 g, 4 mmol) and dimethyl succinate (0.29 g, 2 mmol) was added into a boiling mixture of sodium *tert*-pentoxide (0.75 g, 6.8 mmol) and 8 mL *tert*-amyl alcohol over 1.3 h. The reaction mixture was refluxed for another 2 h and then cooled to room temperature. After adding methanol and concentrated hydrochloric acid, the mixture was stirred for 30 min, and then stood overnight in refrigerator. The precipitate was filtered and washed with methanol and water, to afford crude product **S2** (0.65g), which was used directly in subsequent reactions without further purification.

Synthesis of DPPTT-H

A mixture of **S2** (1.28 g, 2 mmol), K_2CO_3 (1.1 g, 8 mmol) and dry DMF (20 mL) was stirred at 120 °C for 4 h before 1-bromohexane (0.77 g, 4.6 mmol) was added. Then the reaction

mixture was heated at 130 °C for another 2 h and cooled to room temperature. Water was added and the reaction solution was extracted with CHCl_3 . Solvent was removed under vacuum and the residue was purified by column chromatography (CH_2Cl_2 -petroleum ether, 1.5:1) to yield 0.3 g of **DPPTT-H** as a dark blue solid (18.7%); mp. 231 °C; $^1\text{H NMR}$ (CDCl_3) δ 8.90 (d, 2H); 7.22 (d, 2H); 7.13 (d, 2H); 6.72 (d, 2H); 4.06 (t, 4H); 2.8 (t, 4H); 1.64-1.78 (m, 8H); 1.3-1.46 (m, 16H); 0.88 (t, 12H); MS (MALDI-TOF): m/z 801.3; Anal Calcd for $\text{C}_{46}\text{H}_{60}\text{N}_2\text{O}_2\text{S}_4$: C 68.95%, H 7.55%, N 3.50%; Found: C 68.75%, H 7.40% N 3.43%.

Synthesis of DPPTT-F

A 50 mL Schlenk tube was charged with **S3** (1 g, 1.76 mmol), **S4** (0.11 g, 0.176 mmol), $\text{Pd}(\text{PPh}_3)_4$ (10 mg, 0.0087 mmol) and 10 mL toluene. The mixture was stirred at 130 °C for 20 h and then cooled to room temperature. The solid was filtered, washed with CH_2Cl_2 and purified by recrystallization from *o*-dichlorobenzene to afford 0.2g (89.6%) **DPPTT-F** as a dark blue solid; mp. 255 °C; $^1\text{H NMR}$ ($\text{C}_2\text{Cl}_4\text{D}_2$) δ 8.70 (d, 2H); 7.32 (m, 4H); 7.23 (d, 2H); 3.99 (t, 4H); 1.70 (m, 4H); 1.28-1.37 (m, 12H); 0.83 (t, 6H); MS (MALDI-TOF): m/z 1269.5; Anal Calcd for $\text{C}_{46}\text{H}_{34}\text{F}_{26}\text{N}_2\text{O}_2\text{S}_4$: C 43.54%, H 2.70%, N 2.21%; Found: C 43.83%, H 2.91% N 2.12%.

Device Fabrication and characterization

The transistors were fabricated in a top contact, bottom gate configuration. Heavily N-doped Si and a 300 nm thick SiO_2 layer were used as gate electrode and dielectric layer. The specific capacitance of the dielectric layer was 10 nF/cm^2 . The substrates were cleaned and modified with OTS according to reported procedure.²⁵ The **DPPTT-H** and **DPPTT-F** thin films were evaporated on the substrates under 10^{-7} Torr at different substrate temperatures from 25 °C to 85 °C, and the thickness of the films was 50 nm measured by a quartz crystal microbalance. The gold source/drain electrodes were deposited on the semiconductor layer by thermal evaporation using a shadow mask. The channel width and length of the transistors were 273 and 31 μm

respectively. The electrical characterization of the devices was performed by using a Keithley 4200 semiconductor parameter analyzer in air at room temperature.

Results and discussion

The synthetic routes of **DPPTT-H** and **DPPTT-F** are outlined in Scheme 2. Compound **S1** reacted with diethyl succinate in the presence of sodium *tert*-amyl alcohol to afford compound **S2**. Alkylation of compound **S2** with hexyl bromide gave target compound **DPPTT-H** as a dark blue solid. The synthesis of **DPPTT-F** was accomplished by a Still coupling of **S4** and stannic compound **S3**, and the product was purified by recrystallization from *o*-dichlorobenzene. **DPPTT-H** has good solubility in common organic solvents, while **DPPTT-F** was poor soluble in organic solvents, suggesting the different effect of perfluorohexyl and hexyl substituents. Both compounds were fully characterized by ¹HNMR, MS and elemental analysis.

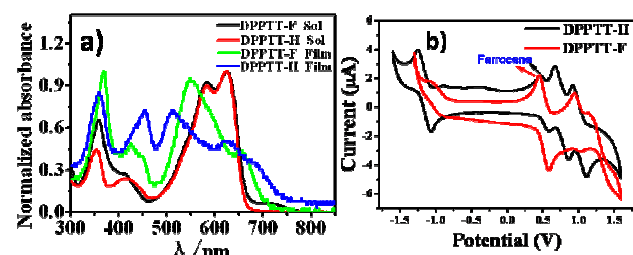


Figure 1. a) UV-vis absorption spectra of **DPPTT-H** and **DPPTT-F** in *o*-dichlorobenzene solution (10^{-6} mol/L) and on thin films (50 nm thickness, deposited on a quartz substrate at 55 °C); b) Cyclic voltammetry of **DPPTT-H** and **DPPTT-F** in *o*-dichlorobenzene solution. 0.1 M Bu_4NPF_6 as electrolyte, SCE as reference electrode, Pt as working electrode.

The UV-vis absorption spectra of **DPPTT-H** and **DPPTT-F** in *o*-dichlorobenzene solution and on thin films are shown in Figure 1. Both compounds have strong absorption in the range of 460–780 nm in solution. Though perfluorohexyl chain has stronger electron withdrawing ability than that of hexyl group, surprisingly **DPPTT-H** and **DPPTT-F** displayed nearly the same absorption spectra in the solution, suggesting the replacement of perfluorohexyl group does not affect the HOMO-LUMO energy gap of the molecules. The optical energy gap estimated from solution spectra is about 1.89 eV. Comparing with that of solution, the absorptions of **DPPTT-H** and **DPPTT-F** based thin films were largely blue shifted. The maximum absorptions of **DPPTT-H** and **DPPTT-F** were blue shifted ~113 nm and 76 nm respectively, indicating strong intermolecular interactions exist in the solid state. Additionally, a shoulder absorption at 630 nm for **DPPTT-H** and at 650 nm for **DPPTT-F** was observed, suggesting both compounds form H-type aggregation in the solid

state.

The cyclic voltammograms (CV) of **DPPTT-H** and **DPPTT-F** were measured in *o*-dichlorobenzene solution with 0.1 M Bu_4NPF_6 as electrolyte, Pt electrode as working electrode, and ferrocene as internal standard (Figure 1b). **DPPTT-H** showed three reversible redox peaks, and the first reduction and oxidation potentials estimated from the midpoint of forward and backward scan are -1.18 V and 0.76 V respectively. The CV of **DPPTT-F** displayed non-reversible redox behavior, which might be ascribed to the effect of perfluorohexyl groups and the low solubility of **DPPTT-F**. The first oxidation and reduction peaks of **DPPTT-F** are at 0.98 V and -1.05 V. The HOMO/LUMO energy levels calculated from CV are -5.03/-3.09 eV for **DPPTT-H** and -5.25 eV/-3.22 eV for **DPPTT-F**. The HOMO-LUMO energy bandgap estimated from electrochemistry is 1.92 eV for **DPPTT-H** and 1.97 eV for **DPPTT-F**, close to the optical bandgap calculated from UV. Apparently, the perfluorohexyl groups lower the HOMO and LUMO energy levels of **DPPTT-F**, but nearly has no influence on its HOMO-LUMO energy bandgap.

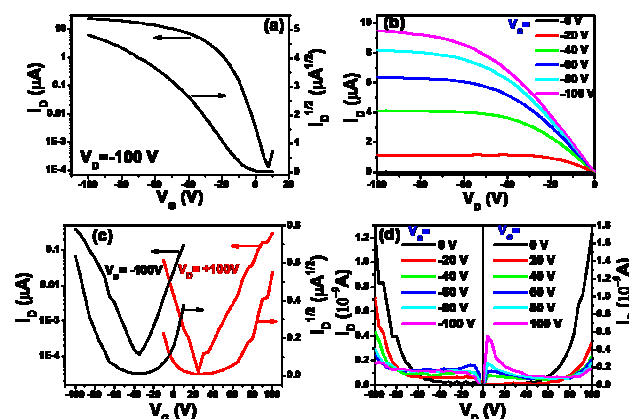


Figure 2. Transfer and output curves of **DPPTT-H** (a, b) and **DPPTT-F** (c, d) based transistors.

In order to investigate the charge transport property of **DPPTT-H** and **DPPTT-F**, top-contact, bottom gate transistors were fabricated. The mobility of devices was calculated in saturation regime according to the expression $I_{\text{DS}} = (W/2L) \mu \times C_i (V_{\text{G}} - V_{\text{Th}})^2$, where L and W are the channel length and width, respectively; C_i is the capacitance. Figure 2 shows the typical transfer and output curves of **DPPTT-H** and **DPPTT-F** based transistors, and their device performance is summarized in Table 1. **DPPTT-H** exhibited p-channel behavior, and the highest hole mobility could reach $\sim 0.2 \text{ cm}^2 \text{V}^{-1} \text{s}^{-1}$ with $I_{\text{on}}/I_{\text{off}}$ ratio $> 10^4$ at substrate temperature (T_{sub}) = 25 °C. When the T_{sub} was increased

Table 1 Field-effect characteristics of **DPPTT-H** and **DPPTT-F** deposited at various substrate temperatures

T_{sub} [°C]	DPPTT-H			DPPTT-F		
	μ_{max} (μ_{aver}) [$\text{cm}^2 \text{V}^{-1} \text{s}^{-1}$]	$I_{\text{on}}/I_{\text{off}}$	V_{T} [V]	μ_{max} (μ_{aver}) [$\text{cm}^2 \text{V}^{-1} \text{s}^{-1}$]	$I_{\text{on}}/I_{\text{off}}$	V_{T} [V]
25	0.20 (0.15)	5.3×10^4	-7	6.6×10^{-5} (6.5×10^{-5}) (h)	1.1×10^2 (h)	-30 (h)
				4.9×10^{-3} (1.4×10^{-3}) (e)	3.6×10^3 (e)	20 (e)
55	0.19 (0.17)	4.0×10^4	15	1.2×10^{-2} (5.0×10^{-3}) (h)	4.6×10^3 (h)	-72 (h)
				1.1×10^{-2} (4.6×10^{-3}) (e)	8.4×10^3 (e)	70 (e)
85	3.8×10^{-2} (3.0×10^{-2})	2.2×10^5	-30	2.7×10^{-4} (8.5×10^{-5}) (h)	5.0×10^2 (h)	-55 (h)
				2.6×10^{-3} (1.3×10^{-3}) (e)	1.0×10^4 (e)	40 (e)

Cite this: DOI: 10.1039/c0xx00000x

www.rsc.org/xxxxxx

ARTICLE TYPE

to 55 °C, the mobility of the devices was nearly no changed and the threshold voltage was slightly increased. Further increasing the T_{sub} to 85 °C, the mobility of the devices decreased to 0.03 cm^2/Vs . **DPPTT-F** based transistors displayed ambipolar characteristic in air. The hole and electron mobility was 6.6×10^{-5} and $4.9 \times 10^{-3} \text{ cm}^2/\text{Vs}$ at $T_{\text{sub}} = 25 \text{ }^\circ\text{C}$ respectively. Unlike **DPPTT-H**, with the increase of T_{sub} , the performance of **DPPTT-F** increased. The highest performance was observed at $T_{\text{sub}} = 55 \text{ }^\circ\text{C}$, balanced hole and electron mobility up to $10^{-2} \text{ cm}^2\text{V}^{-1}\text{s}^{-1}$ was achieved, one of the highest value for DPP based small molecular ambipolar semiconductors in ambient condition. Absolutely, the perfluoroethyl chains should be responsible for the different electrical behaviors of **DPPTT-H** and **DPPTT-F**. Moreover, **DPPTT-F** based ambipolar transistors can be operated in air though the LUMO energy level of **DPPTT-F** is -3.22 eV, further demonstrating the unique property of perfluoroalkyl chains and their potential applications in high performance organic ambipolar semiconductors. In addition, the low optimized substrate temperature (55 °C) guarantees the potential applications of these compounds in flexible transistors.

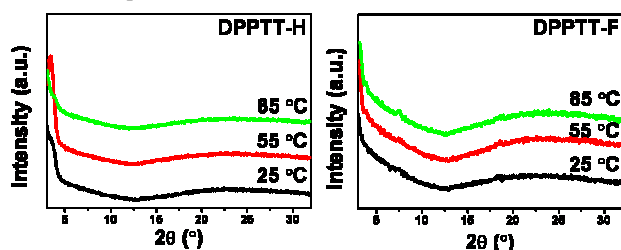


Figure 3. X-Ray diffraction of **DPPTT-H** and **DPPTT-F** films deposited on OTS modified Si/SiO₂ substrates at different substrate temperatures. The wavelength for the X-Ray source is 0.154 nm.

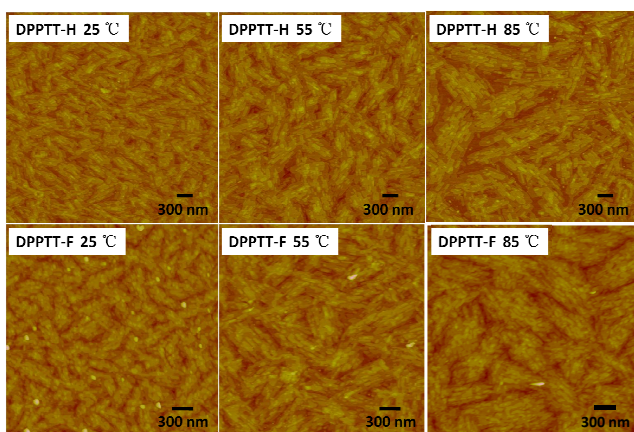


Figure 4. AFM images of **DPPTT-H** ($4 \times 4 \mu\text{m}^2$) and **DPPTT-F** ($3 \times 3 \mu\text{m}^2$) thin films deposited on OTS modified Si/SiO₂ substrates at different substrate temperature.

The thin film quality, microstructure and morphology of **DPPTT-H** and **DPPTT-F** were investigated by X-ray diffraction (XRD) and atomic force microscopy (AFM). Figure 3 illustrates

the XRD patterns of the thin films deposited at different substrate temperatures. **DPPTT-H** thin films showed one diffraction peak when the T_{sub} was 25 °C and 55 °C respectively. The d-spacing estimated from XRD is 2.36 nm at $T_{\text{sub}} = 25 \text{ }^\circ\text{C}$ and 2.59 nm at $T_{\text{sub}} = 55 \text{ }^\circ\text{C}$, suggesting **DPPTT-H** adopts different packing models on the substrate. Surprisingly, this changes has nearly no influence on the mobility and just slightly affected the threshold voltage of the devices, indicating both molecular packing models of **DPPTT-H** favorite charge transport. It is known the threshold voltage is strongly affected by the traps in the interfaces such as organic semiconductor - electrodes interface and organic semiconductor - dielectric layer interface, and in organic semiconductor thin film. We believe, more traps were formed in the devices at $T_{\text{sub}} = 55 \text{ }^\circ\text{C}$, which led to the increase of the threshold voltage. No peaks were observed for the films deposited at 85 °C, indicating its less crystalline and being consistent with the device performance. For **DPPTT-F** thin films, a series of single family diffraction peaks were observed. With the increase of substrate temperature, the intensity of the peaks increased, indicating the improved crystalline of the films. The d-spacing estimated from the first diffraction peak is 2.33 nm, close to that of **DPPTT-H** thin film deposited at $T_{\text{sub}} = 25 \text{ }^\circ\text{C}$. Figure 4 shows the AFM images of **DPPTT-H** and **DPPTT-F** thin films. With increasing the substrate temperature from 25 °C to 55 °C, the grain size of **DPPTT-F** increased, and the grain boundaries became larger. While the substrate temperature increased to 85 °C, the grain size as well as grain boundary further increased, and the continuity of the film became worse. The thin films with large grain sizes and short grain boundaries facilitate charge transport. The large grain boundary might be responsible for the deteriorated device performance of **DPPTT-F** at $T_{\text{sub}} = 85 \text{ }^\circ\text{C}$. The morphology of **DPPTT-H** thin films exhibited the same tendency as that of **DPPTT-F** with the increase of substrate temperature. The different crystalline and morphology of the thin films led to the performance variation of **DPPTT-H** and **DPPTT-F** films at different substrate temperatures.

Conclusions

In summary, two novel DPP based small molecules, **DPPTT-H** and **DPPTT-F** were prepared. Their physicochemical properties were investigated by absorption spectra and electrochemistry. Comparing with **DPPTT-H**, the HOMO and LUMO energy levels of **DPPTT-F** lowered, but the HOMO-LUMO bandgap was nearly the same, demonstrating the unique effect of perfluoroalkyl substituents to the energy levels of the frontier orbital of compounds. Thin film transistor characteristics showed **DPPTT-H** displayed p-channel behavior with hole mobility of $0.2 \text{ cm}^2\text{V}^{-1}\text{s}^{-1}$. And **DPPTT-F** exhibited ambipolar characteristics with balanced hole and electron mobility in air. The maximum hole and electron mobility of **DPPTT-F** was 0.012 and $0.011 \text{ cm}^2\text{V}^{-1}\text{s}^{-1}$ respectively, which was observed at $T_{\text{sub}} = 55 \text{ }^\circ\text{C}$, one of the highest and balanced value for DPP based small molecules

in air. AFM image and XRD results showed the morphology and crystalline changes are responsible for the mobility variation of DPPTT-H and DPPTT-F at different substrate temperatures.

Acknowledgements

This work was supported by National Natural Sciences Foundation of China (21190031, 51273212) and National Basic Research Program of China (2011CB808405).

Notes and references

^a Shanghai Institute of Organic Chemistry, Shanghai, 200032, China. E-mail: lhx@mail.sioc.ac.cn

^b State Key Laboratory of Crystal Materials, Shandong University, Jinan, 250100, China. E-mail: zqliu@sdu.edu.cn

† These authors contributed equally.

1. M. Tantiwiwat, A. Tamayo, N. Luu, X.-D. Dang, T.-Q. Nguyen, *J. Phys. Chem. C* 2008, **112**, 17402.
2. L. Bürgi, M. Turbiez, R. Pfeiffer, F. Bienewald, H.-J. Kirner, C. Winnewisser, *Adv. Mater.*, 2008, **20**, 2217.
3. J. C. Bijleveld, A. P. Zoombelt, S. G. J. Mathijssen, M. M. Wienk, M. Turbiez, D. M. de Leeuw, R. A. J. Janssen, *J. Am. Chem. Soc.*, 2009, **131**, 16616.
4. L. Huo, J. Hou, H.-Y. Chen, S. Zhang, Y. Jiang, T. L. Chen and Y. Yang, *Macromolecules*, 2009, **42**, 6564.
5. P. Sonar, S. P. Singh, Y. Li, M. S. Soh, A. Dodabalapur, *Adv. Mater.*, 2010, **22**, 5409.
6. Z. Chen, M. J. Lee, R. S. Ashraf, Y. Gu, S. Albert-Seifried, M. M. Nielsen, B. Schroeder, T. D. Anthopoulos, M. Heeney, I. McCulloch, H. Sirringhaus, *Adv. Mater.*, 2012, **24**, 647.
7. J. D. Yuen, J. Fan, J. Seifert, B. Lim, R. Hufschmid, A. J. Heeger, F. Wudl, *J. Am. Chem. Soc.*, 2011, **133**, 20799.
8. S. Cho, J. Lee, M. Tong, J. H. Seo, C. Yang, *Adv. Funct. Mater.*, 2011, **21**, 1910.
9. S. Loser, C. J. Bruns, H. Miyauchi, R. P. Ortiz, A. Facchetti, S. I. Stupp, T. J. Marks, *J. Am. Chem. Soc.*, 2011, **133**, 8142.
10. R. Mohebbi, J. Yuen, J. Fan, C. Munoz, M. Wang, R. S. Shirazi, J. Seifert, F. Wudl, *Adv. Mater.*, 2011, **23**, 4644.
11. H. Bronstein, Z. Chen, R. S. Ashraf, W. Zhang, J. Du, J. R. Durrant, P. S. Tuladhar, K. Song, S. E. Watkins, Y. Geerts, M. M. Wienk, R. A. J. Janssen, T. Anthopoulos, H. Sirringhaus, M. Heeney, I. McCulloch, *J. Am. Chem. Soc.*, 2011, **133**, 3272.
12. B. Walker, A. B. Tomayo, X.-D. Dang, P. Zalar, J. H. Seo, A. Garcia, M. Tantiwiwat, T.-Q. Nguyen, *Adv. Funct. Mater.*, 2009, **19**, 3063.
13. P. Sonar, G.-M. Ng, T. T. Lin, A. Dodabalapur, Z.-K. Chen, *J. Mater. Chem.*, 2010, **20**, 3626.
14. S.-L. Suraru, U. Zschieschang, H. Klauk, F. Würthner, *Chem. Commun.*, 2011, **47**, 1767.
15. H. Zhong, J. Smith, S. Rossbauer, A. J. P. White, T. D. Anthopoulos, M. Heeney, *Adv. Mater.*, 2012, **24**, 3205.
16. Y. Zhang, C. Kim, J. Lin, T.-Q. Nguyen, *Adv. Funct. Mater.*, 2012, **22**, 97.
17. J. Lee, A.-R. Han, J. Kim, Y. Kim, J. H. Oh, C. Yang, *J. Am. Chem. Soc.*, 2012, **134**, 20713.
18. J. H. Park, E. H. Jung, J. W. Jung, W. H. Jo, *Adv. Mater.*, 2013, **25**, 2583.
19. P. Sonar, G.-M. Ng, T. T. Lin, A. Dodabalapur, Z.-K. Chen, *J. Mater. Chem.*, 2010, **20**, 3626.
20. S. Liu, M. Shi, J. Huang, Z. Jin, X. Hu, J. Pan, H. Li, A. K.-Y. Jen, H. Chen, *J. Mater. Chem. A* 2013, **1**, 2795.
21. Facchetti, M. Mushrush, H. E. Katz, T.J.Marks, *Adv. Mater.*, 2003, **15**, 33.
22. Y. Nicolas, P. Blanchard, E. Levillain, M. Allain, N. Mercier, J. Roncali, *Org. Lett.*, 2004, **6**, No. 2, 273.
23. E. Kurach, D. Djurado, J. Rimarcik, A. Kornet, M. Wlostowski, V. Lukes, J. Pécaut, M. Zagorska, A. Pron, *Phys. Chem. Chem. Phys.*, 2011, **13**, 2690.
24. S. P. Mishra, A. K. Palai, M. Patri, *Synth. Met.*, 2010, **160**, 2422.
25. M. Wang, J. Li, G. Zhao, Q. Wu, Y. Huang, W. Hu, X. Gao, H. Li, D. Zhu, *Adv. Mater.* 2013, **25**, 2229.